The Design of Optical Pulse Shapes with an Aperture-Coupled-Stripline Pulse-Shaping System

Laser-fusion experiments require precise control of the temporal profile of optical pulses applied to targets. An optical pulse–shaping system has been in operation on OMEGA for several years.[1] During this time the demands on the precision, flexibility, and repeatability of the optical pulse–shaping system have steadily increased. To meet these new demands, a new pulse-shaping system based on an aperture-coupled stripline (ACSL) electrical-waveform generator has been developed and discussed previously.[2] This new system will be implemented on OMEGA in the next few months. In addition to its simplicity, the new system will include significant improvements to the modeling, performance, and diagnostics of the pulse-shaping system to meet the challenging demands required of the system. The shaped optical pulses produced by this system become the seed pulses that are injected into the OMEGA laser system. Details of the on-target pulse shape from the OMEGA laser are critically related to the details of the seed-pulse shape. This article describes the modeling of an ACSL pulse-shaping system that is used to produce an optical seed pulse with a specified temporal shape.

An ACSL generates temporally shaped electrical waveforms that are applied to electro-optic modulators to produce shaped optical pulses. The electro-optic modulators exhibit a finite response time to an applied voltage. This response time has been measured and is included in the calculation of the voltage waveform required from the ACSL to produce a specific optical pulse shape. An ACSL is modeled as two coupled and interacting striplines. Striplines are modeled as transmission lines that obey a set of equations known as the telegraph equations.[3] A new approach to solving the telegraph equations using the method of characteristics is presented here along with a straightforward extension of this approach to ACSL's. The modeling presented here leads to a prescription for determining the necessary ACSL geometry to produce a desired on-target pulse shape on OMEGA.

The Optical Modulator Voltage Waveforms

Given the temporal profile of the optical pulse required on target from the OMEGA laser, the temporal profile of the optical seed pulse that must be produced by the pulse-shaping system is determined from the extensive modeling of the laser system that has evolved over the years. As shown in Fig. 78.41, this low-energy optical seed pulse is shaped by applying shaped voltage waveforms to a dual-channel electro-optic amplitude modulator synchronous with the transit through the modulator of an optical pulse from a single-longitudinal-mode (SLM) laser.[4] If we neglect the finite response time of the modulator, the intensity profile of an optical pulse exiting a modulator is given by

$$I_{\text{out}}(t) = I_{\text{in}}(t)\sin^2\left\{\pi/2\left[V_1(t)/V_\pi + \phi_1\right]\right\}$$

$$\times \sin^2\left\{\pi/2\left[V_2(t)/V_\pi + \phi_2\right]\right\}, \qquad (1)$$

where $I_{\text{in}}(t)$ is the intensity profile of the optical pulse sent into the modulator from the SLM laser; the two sine-squared factors represent the transmission functions of the two modulator channels with $V_1(t)$ the voltage waveform applied to channel 1 of the modulator, $V_2(t)$ the voltage waveform applied to channel 2 of the modulator, V_π the half-wave voltage of the modulator (typically less than 10 V), and ϕ_1 and ϕ_2 the offsets

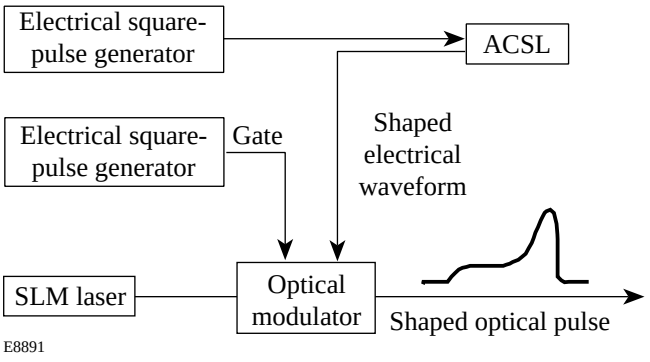

Figure 78.41
The aperture-coupled-stripline (ACSL) optical pulse–shaping system. The output from an electrical square-pulse generator is temporally shaped by an ACSL and used to drive an optical modulator. A separate electrical square-pulse generator is used to gate the second channel of the modulator.

set to zero by the application of a dc bias to each of the modulator channels. The input intensity profile to the modulator is assumed to be unity for our application since the short-duration (<5 ns) voltage waveforms $V_1(t)$ and $V_2(t)$ are applied to the modulators during the peak of the 200-ns Gaussian optical pulse from the SLM laser.

On one channel of the modulator, a shaped electrical waveform from an ACSL is applied. The exact shape of the voltage waveform required from the ACSL is determined by the shape of the optical pulse required from the modulator and by the response of the modulator to an applied voltage. This channel is referred to as the shaping channel of the modulator. On the other channel of the modulator, a square electrical waveform is applied. This channel is intended to produce a square optical waveform that acts as a gate to block unwanted pre- and post-pulses from the modulator and enhances the contrast of the output shaped optical pulse from the modulator. This channel of the modulator is referred to as the gate channel. The optical pulse produced by the gate channel should ideally have a fast rise and fall time with constant amplitude over its duration. The application of a square electrical pulse (with 45-ps rise time) to this channel from a pulse generator (Model 10,050A from Picosecond Pulsed Laboratories, Boulder, CO) produces the optical pulse shape shown in Fig. 78.42. This figure reveals the bandwidth limitations of the modulator for this "ideal" (high-bandwidth) square input electrical pulse. In particular, the optical pulse from this channel does not reach its full amplitude during the first 200 to 300 ps of the pulse, which, if not properly compensated for, can cause pulse distortion on the beginning of a shaped optical pulse and severe pulse distortion for short-pulse generation. This distortion caused by the modulator bandwidth limitation is minimized by including this effect when calculating the voltage waveform applied to the modulator's shaping channel as discussed below.

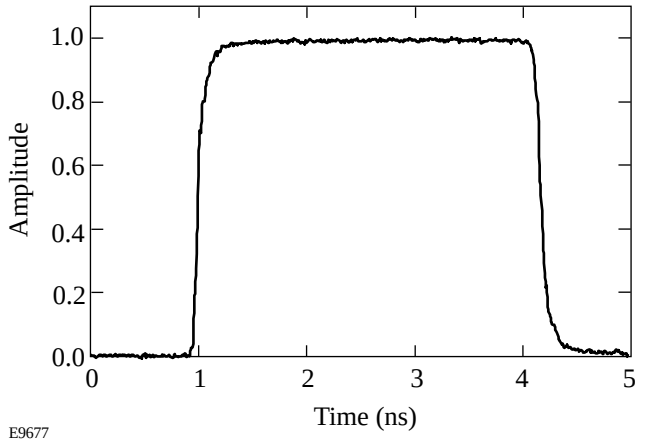

Figure 78.42
The measured optical pulse shape from a single channel of an electro-optic modulator with a square electrical waveform applied to the RF port. The square electrical waveform has a rise time of 45 ps.

Numerical Solution of the Telegraph Equations

Transmission line problems can be classified into two categories. The first category deals with determining the transmission line properties required to produce a specific electrical waveform reflected from the line, given the input electrical waveform to the line. The second category is the reciprocal of the first and deals with determining the electrical waveform reflected from a transmission line, given the input electrical waveform to the line and the properties of the transmission line.

In the present OMEGA pulse-shaping system, shaped electrical waveforms are generated by the reflection from a variable-impedance micro stripline and sent to the shaping channel of the modulator.[2] The micro striplines are designed using a layer-peeling technique that treats the micro stripline as a simple transmission line.[5] This technique allows one to calculate the reflection coefficient along the line (and from that the electrode width) needed to synthesize a given electrical waveform in reflection. The reciprocal of this calculation is to determine the electrical waveform reflected from a transmission line given the reflection coefficient along the line. This latter calculation is discussed here and, in the next section, will be extended to include modeling ACSL's to generate shaped electrical waveforms.

In this section we develop the equations that describe the electrical waveforms propagating along a transmission line starting from the well-known telegraph equations for the line.[3] First we model a stripline or micro stripline as a transmission line that obeys the telegraph equations:

$$\frac{\partial v(x,t)}{\partial x} = -L(x)\frac{\partial i(x,t)}{\partial t}, \tag{2a}$$

$$\frac{\partial i(x,t)}{\partial x} = -C(x)\frac{\partial v(x,t)}{\partial t}, \tag{2b}$$

where v is the voltage along the line, i is the current flowing along the line, L is the inductance per unit length along the line, and C is the capacitance per unit length along the line. In these

equations we introduce the characteristic impedance of the line $Z(x) = \sqrt{L(x)/C(x)}$ and the wave propagation velocity $dx/dt = c = 1/\sqrt{LC}$ along the line. We assume that the propagation velocity c (not to be confused with the speed of light) along the line is constant. With these substitutions Eqs. (2) become

$$\frac{\partial V(x,t)}{\partial x} = -k(x)V(x,t) - c\frac{\partial I(x,t)}{\partial t}, \tag{3a}$$

$$\frac{\partial I(x,t)}{\partial x} = k(x)I(x,t) - c\frac{\partial V(x,t)}{\partial t}, \tag{3b}$$

where the variables are defined as

$$V(x,t) = v(x,t)Z^{-1/2}(x) \tag{4a}$$

and

$$I(x,t) = i(x,t)Z^{1/2}(x) \tag{4b}$$

and where

$$k(x) = \frac{1}{2Z(x)}\frac{dZ(x)}{dx} \tag{5}$$

is the reflection coefficient per unit length along the line.

If we add and subtract Eqs. (3), we get a set of reduced wave equations

$$\frac{\partial WR(x,t)}{\partial x} + \frac{1}{c}\frac{\partial WR(x,t)}{\partial t} = -k(x)WL(x,t) \tag{6a}$$

and

$$\frac{\partial WL(x,t)}{\partial x} + \frac{1}{c}\frac{\partial WL(x,t)}{\partial t} = -k(x)WR(x,t), \tag{6b}$$

where

$$WR(x,t) = \left[V(x,t) + I(x,t)\right]/2$$

$$= \left[v(x,t)Z^{-1/2}(x) + i(x,t)Z^{1/2}(x)\right]/2 \tag{7a}$$

is a wave traveling to the right along the line with velocity c and

$$WL(x,t) = \left[V(x,t) - I(x,t)\right]/2$$

$$= \left[v(x,t)Z^{-1/2}(x) - i(x,t)Z^{1/2}(x)\right]/2 \tag{7b}$$

is a wave traveling to the left along the line with velocity c. In the appendix we show that the form of Eqs. (6) is identical to the form of the equation obtained if one substitutes a plane wave with slowly varying amplitude into the wave equation. Therefore, Eqs. (6) are referred to as the reduced wave equations and are the main results of this section. In the next section we show how to extend these equations to model an ACSL and give a numerical prescription for solving the resulting equations using the method of characteristics.

Extension to an ACSL

The geometry of an ACSL is shown in Fig. 78.43. In principle, an ACSL is a directional coupler consisting of two striplines that are coupled through an aperture in their common ground plane. In operation, a square electrical waveform is launched into port 1 and propagates along electrode 1 to the terminated port 2 of the ACSL. As the square electrical waveform propagates along electrode 1 in the coupling region, a signal is coupled through an aperture to electrode 2 in the backward direction and exits at port 4. The electrical waveform exiting port 4 is sent to the shaping channel of the modulator and must have the proper temporal profile to produce the desired optical pulse shape out of the modulator. By varying the width of the coupling aperture (shown in Fig. 78.43) along the length of the ACSL, a temporally shaped electrical waveform can be generated at port 4. The details of how to calculate the width of this aperture along the line to produce a specific electrical waveform from the ACSL are the main topic of this article.

The ACSL is modeled as two coupled transmission lines. We can extend the formalism in the previous section to an ACSL by writing four reduced wave equations. Two equations describe the waves WR1(x,t) and WR2(x,t) traveling to the right along lines 1 and 2, respectively, and two equations describe the waves WL1(x,t) and WL2(x,t) traveling to the left along lines 1 and 2, respectively. In each reduced wave equation we include the reflection coefficient $k(x)$ along the line as above, and we introduce a coupling term $C(x)$ that allows for coupling waves from one line to the other through the aperture.

The resulting equations are given by

$$\frac{\partial \mathrm{WR1}(x,t)}{\partial x} + \frac{1}{c}\frac{\partial \mathrm{WR1}(x,t)}{\partial t} = -k(x)\,\mathrm{WL1}(x,t) - C(x)\,\mathrm{WL2}(x,t), \tag{8a}$$

$$\frac{\partial \mathrm{WL1}(x,t)}{\partial x} - \frac{1}{c}\frac{\partial \mathrm{WL1}(x,t)}{\partial t} = -k(x)\,\mathrm{WR1}(x,t) - C(x)\,\mathrm{WR2}(x,t), \tag{8b}$$

$$\frac{\partial \mathrm{WR2}(x,t)}{\partial x} + \frac{1}{c}\frac{\partial \mathrm{WR2}(x,t)}{\partial t} = -k(x)\,\mathrm{WL2}(x,t) - C(x)\,\mathrm{WL1}(x,t), \tag{8c}$$

$$\frac{\partial \mathrm{WL2}(x,t)}{\partial x} - \frac{1}{c}\frac{\partial \mathrm{WL2}(x,t)}{\partial t} = -k(x)\,\mathrm{WR2}(x,t) - C(x)\,\mathrm{WR1}(x,t). \tag{8d}$$

The coupling coefficient $C(x)$ is the coupling from one line to the other in the backward direction. In general, another coupling term should be added to the above equations to model coupling from one line to the other in the forward direction. This forward coupling term can be trivially added to this model; however, for directional couplers of this sort, coupling in the forward direction is negligible.

The reduced wave equations (8) for an ACSL [as well as Eqs. (6) for striplines] can be solved by transforming them along the characteristic curves

$$\xi = ct - x \quad \text{and} \quad \eta = ct + x. \tag{9}$$

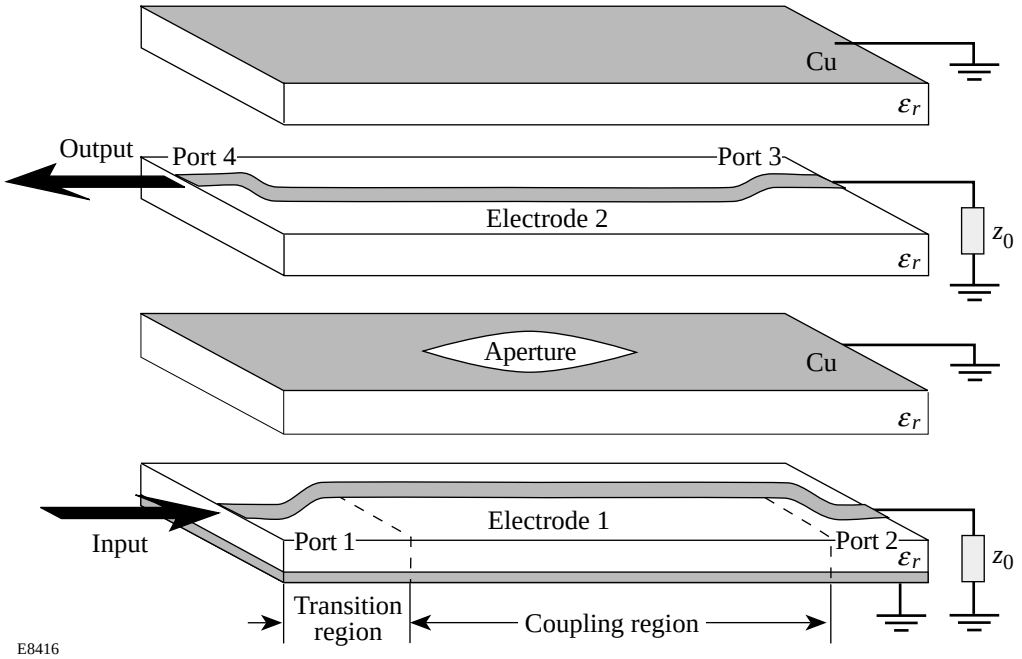

Figure 78.43
Exploded view of a practical four-layer, four-port ACSL. A square electrical waveform is launched into port 1 and propagates along electrode 1 to the terminated port 2. An electrical signal is coupled through an aperture to electrode 2 in the backward direction, and a shaped electrical waveform exits at port 4.

For this transformation we use the chain rules

$$\frac{\partial}{\partial x}=\frac{\partial}{\partial \xi}\frac{\partial \xi}{\partial x}+\frac{\partial}{\partial \eta}\frac{\partial \eta}{\partial x}=\left(-\frac{\partial}{\partial \xi}+\frac{\partial}{\partial \eta}\right) \tag{10a}$$

and

$$\frac{\partial}{\partial t}=\frac{\partial}{\partial \xi}\frac{\partial \xi}{\partial t}+\frac{\partial}{\partial \eta}\frac{\partial \eta}{\partial t}=c\left(\frac{\partial}{\partial \xi}+\frac{\partial}{\partial \eta}\right) \tag{10b}$$

to obtain

$$\frac{\mathrm{dWR1}(\eta)}{\mathrm{d}\eta}=-\left[k(x)\mathrm{WL1}(\xi)+C(x)\,\mathrm{WL2}(\xi)\right]/2, \tag{11a}$$

$$\frac{\mathrm{dWL1}(\xi)}{\mathrm{d}\xi}=\left[k(x)\,\mathrm{WR1}(\eta)+C(x)\,\mathrm{WR2}(\eta)\right]/2, \tag{11b}$$

$$\frac{\mathrm{dWR2}(\eta)}{\mathrm{d}\eta}=-\left[k(x)\mathrm{WL2}(\xi)+C(x)\mathrm{WL1}(\xi)\right]/2, \tag{11c}$$

$$\frac{\mathrm{dWL2}(\xi)}{\mathrm{d}\xi}=\left[k(x)\mathrm{WR2}(\eta)+C(x)\mathrm{WR1}(\eta)\right]/2, \tag{11d}$$

where we have used the fact that WR1,2 are waves propagating in the positive x direction and WL1,2 are waves propagating in the negative x direction and obey wave equations with solutions of the form

$$\mathrm{WR1,2}(x,t)=\mathrm{WR1,2}(ct+x)=\mathrm{WR1,2}(\eta) \tag{12a}$$

and

$$\mathrm{WL1,2}(x,t)=\mathrm{WL1,2}(ct-x)=\mathrm{WL1,2}(\xi). \tag{12b}$$

With this transformation the derivatives in Eqs. (11) become total derivatives.

The coordinate transformation expressed by Eqs. (9) lends itself to a simple geometric interpretation that leads to a numerical solution algorithm for the reduced-wave Eqs. (11). The transformation Eqs. (9) with $\mathrm{d}x = c\mathrm{d}t$ can be seen to be a rotation of the x,ct coordinate system by 45° into the ξ,η coordinate system as shown in Fig. 78.44. In the new ξ,η coordinate system, Eqs. (11) describe how the right-going waves WR1,2 evolve in the η direction and how the left-going waves WL1,2 evolve in the ξ direction. The differential element in this new system is seen to be

$$\mathrm{d}\eta=\frac{\partial \eta}{\partial x}\mathrm{d}x+\frac{\partial \eta}{\partial t}\mathrm{d}t=\mathrm{d}x+c\mathrm{d}t=2\mathrm{d}x, \tag{13}$$

where we have used $\mathrm{d}x = c\mathrm{d}t$. To solve Eqs. (11) numerically, we define a matrix as shown in Fig. 78.44 for each of the four waves and write the finite difference equations

$$\mathrm{WR1}(i,j)=\mathrm{WR1}(i-1,j-1)$$

$$-\left[k(i)\,\mathrm{WL1}(i+1,j-1)+C(i)\,\mathrm{WL2}(i+1,j-1)\right]\mathrm{d}x, \tag{14a}$$

$$\mathrm{WL1}(i,j)=\mathrm{WL1}(i+1,j-1)$$

$$-\left[k(i)\,\mathrm{WR1}(i-1,j-1)+C(i)\,\mathrm{WR2}(i+1,j-1)\right]\mathrm{d}x, \tag{14b}$$

$$\mathrm{WR2}(i,j)=\mathrm{WR2}(i-1,j-1)$$

$$-\left[k(i)\,\mathrm{WL2}(i+1,j-1)+C(i)\,\mathrm{WL1}(i+1,j-1)\right]\mathrm{d}x, \tag{14c}$$

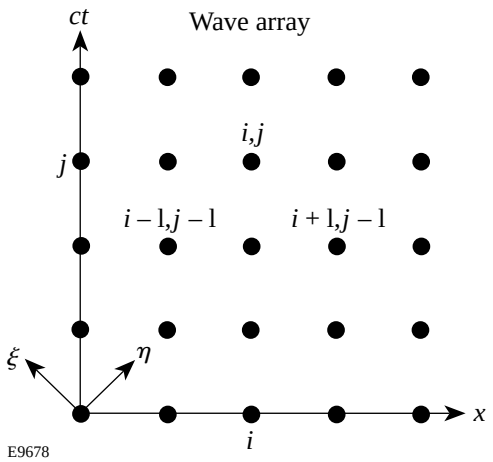

Figure 78.44
An array used by the numerical solution technique to represent a wave propagating along a transmission line. The value at each location in the array gives the amplitude of the wave at some fixed position along the line at some time. Four such arrays are used in the calculation to represent the four waves propagating in an ACSL.

$$\mathrm{WL2}(i,j) = \mathrm{WL2}(i+1, j-1)$$

$$-\left[k(i)\,\mathrm{WR2}(i-1, j-1) + C(i)\,\mathrm{WR1}(i+1, j-1)\right]\mathrm{d}x, \quad (14\mathrm{d})$$

where the index i represents the position x along the line and the index j represents the time t. In these equations, for example, the value of the matrix element at the location i,j in the WR1 array is the amplitude of the wave WR1 at position x along the line at time t. Equations (14) give the values of the four waves at some time, given values of the waves at an earlier time and the reflection and coupling coefficients (k and C) along the line. Therefore, given the coupling coefficients and the initial values of the waves along the line (at $j = 0$ for all i) and the values of the waves at the boundaries for all time (at the first and last i value for all j), Eqs. (14) can be used to find all other values in the arrays. Knowing all values in the four arrays determines the amplitudes of the four waves at all locations along the line for all time. In particular, we specify the right-going wave on line 1 (the pulse from the pulse generator applied to port 1), and we calculate the left-going wave on line 2 (the pulse at port 4 that is applied to the modulator shaping channel). In the next section we show how to apply this technique to the design of optical pulse shapes from the ACSL pulse-shaping system.

Optical Pulse Shape Design/Performance

It is important to use actual measured waveforms or accurately modeled waveforms as input to the pulse-shaping model whenever possible to compensate for imperfections introduced by these waveforms that cannot be corrected by other means. The temporally shaped voltage waveform [V_2 in Eq. (1)] that must be produced by the ACSL and applied to the pulse-shaping channel of the modulator is calculated from Eq. (1). In Eq. (1), I_{out} is the desired temporally shaped optical pulse from the modulator, and the gate channel transmission function is modeled after data similar to that shown in Fig. 78.42. With these substitutions in Eq. (1), the required voltage waveform V_2 is determined, and an ACSL can be designed and fabricated to produce this voltage waveform.

The numerical solution described in the previous section allows one to calculate the electrical waveforms from all four ports of an ACSL given the reflection coefficient $k(x)$ and coupling coefficient $C(x)$ along the line. Experiments show that for any aperture width along the line, these coefficients are equal at each point along the line. To obtain a first approximation to these coefficients a modified version of the layer-peeling technique[5] is used. In the modified layer-peeling technique, the effective reflection coefficient at each point along the line is calculated given the desired output electrical waveform from port 4 and given an ideal input square electrical pulse (i.e., square pulse with an infinite bandwidth) applied to port 1 of the ACSL. (The layer-peeling technique, unfortunately, has difficulties when using an actual measured electrical waveform as input to the line.) Using this first approximation for the reflection and coupling coefficients and using the measured electrical square pulse from the square-pulse generator (Model 4500E from Picosecond Pulsed Laboratories) as input to port 1 of the ACSL, the shaped voltage waveform exiting port 4 of the ACSL is calculated as described in the previous section. This calculated electrical waveform from port 4 of the ACSL is then compared to the required electrical waveform V_2 from this port; this comparison is then used to derive a second approximation to the coupling coefficients. This iteration process can be continued until the calculated output waveform from port 4 of the ACSL is identical to the required output waveform to any degree of accuracy (in practice, one iteration gives sufficient accuracy). Once the coupling coefficient C is determined in this way, the aperture width along the line is obtained from the relationship of the aperture width to the coupling coefficient shown in Fig. 78.45.[2]

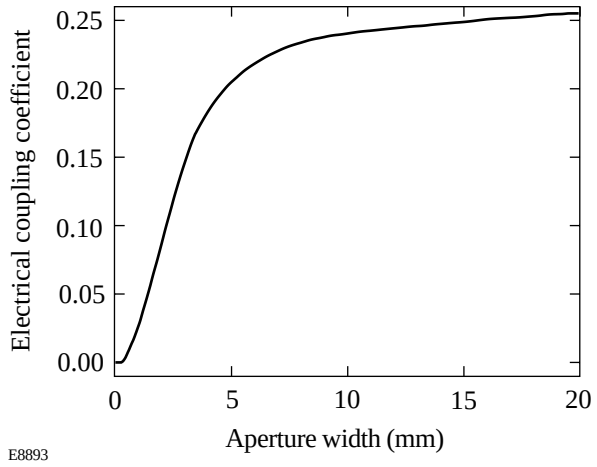

Figure 78.45
The electrical coupling coefficient, defined as the ratio of the output voltage at port 4 to the input voltage applied to port 1 shown in Fig. 78.43, plotted as a function of aperture width for an ACSL with the geometry discussed in the text.

Figure 78.46 shows the design of a specific pulse shape for the OMEGA laser. In Fig. 78.46(a), the design voltage waveform V_2 is compared to the measured voltage waveform from port 4 of the fabricated ACSL. In Fig. 78.46(b), the design optical waveform required from the modulator is compared

to the measured optical waveform from the modulator. Figure 78.46(c) shows the predicted on-target OMEGA UV pulse shape calculated from the measured optical pulse shape from the modulator [Fig. 78.46(b)] and compared to the desired on-target OMEGA UV pulse shape.

Summary

In conclusion, an ACSL pulse-shaping system will be implemented on OMEGA. A model has been developed that allows one to produce accurately shaped optical pulses suitable for injection into the OMEGA laser system. The ACSL electrical-waveform generator is modeled with a numerical solution of the telegraph equations using the method of characteristics. The model uses as input the measured electrical square pulse from the pulse generator used in the pulse-shaping system. The model also compensates for the pulse-shape distortion due to bandwidth limitations of the modulator introduced primarily by the gate pulse. The ACSL pulse-shaping system is a significant improvement over the existing pulse-shaping system currently on OMEGA because of its simplicity, enhanced performance and diagnostics, and improved modeling capabilities.

ACKNOWLEDGMENT

The authors acknowledge the support of the staff at the Laboratory for Laser Energetics of the University of Rochester without whose many years of diligent work the OMEGA laser system would not exist. This work was supported by the U.S. Department of Energy Office of Inertial Confinement Fusion under Cooperative Agreement No. DE-FC03-92SF19460, the University of Rochester, and New York State Energy Research and Development Authority. The support of DOE does not constitute an endorsement by DOE of the views expressed in this article.

Appendix A: Derivation of the Reduced Wave Equation

In this appendix we derive the reduced wave equation that results by substituting a plane wave with slowly varying amplitude into the wave equation. For simplicity, we assume that the

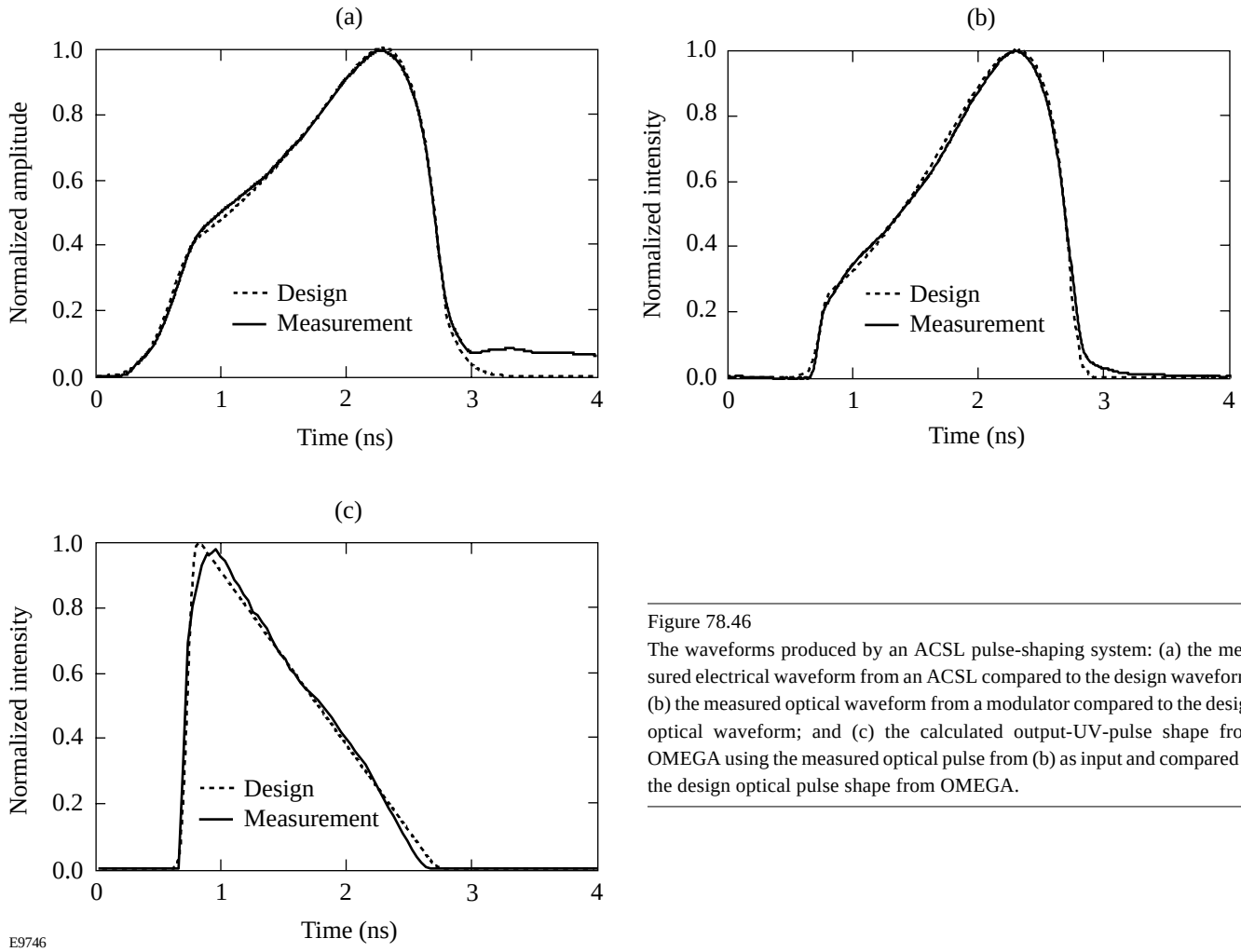

Figure 78.46
The waveforms produced by an ACSL pulse-shaping system: (a) the measured electrical waveform from an ACSL compared to the design waveform; (b) the measured optical waveform from a modulator compared to the design optical waveform; and (c) the calculated output-UV-pulse shape from OMEGA using the measured optical pulse from (b) as input and compared to the design optical pulse shape from OMEGA.

wave is linearly polarized and propagating in the x direction in a nondispersive medium. The plane wave can be represented by

$$E_{\pm}(x,t) = A_{\pm}(x,t)\exp\left[i(\omega t \mp kx)\right] + \text{cc}, \qquad \text{(A1)}$$

where $A_{\pm}$ is the complex amplitude of the wave, the upper sign representing a wave propagating to the right and the lower sign representing a wave propagating to the left; $\omega = 2\pi\nu$ is the angular frequency of the wave with frequency ν; $k = 2\pi/\lambda$ is the propagation constant of the wave with wavelength λ; and cc implies complex conjugate. The purpose of representing the waves in this form is to factor out the slow variations (the temporal profile of the electrical waveform) from the rapid oscillations (referenced to some microwave carrier frequency $\omega/2\pi$). The one-dimensional wave equation is given by

$$\frac{\partial^2 E_{\pm}(x,t)}{\partial x^2} - \frac{1}{c^2}\frac{\partial^2 E_{\pm}(x,t)}{\partial t^2} = 0, \qquad \text{(A2)}$$

where $c = \omega/k$ is the velocity of the wave. If we substitute A1 into A2, after some manipulation we get

$$\frac{\partial^2 A_{\pm}}{\partial x^2} \mp 2ik\frac{\partial A_{\pm}}{\partial x} - \frac{1}{c^2}\frac{\partial^2 A_{\pm}}{\partial t^2} + 2i\frac{\omega}{c^2}\frac{\partial A_{\pm}}{\partial t} = 0, \qquad \text{(A3)}$$

where we have used $c = \omega/k$ to eliminate terms. We now use the fact that the amplitude is slowly varying, that is

$$\frac{\partial A_{\pm}}{\partial x} << \left| kA_{\pm} \right| \qquad \text{(A4a)}$$

and

$$\frac{\partial A_{\pm}}{\partial t} << \left| \omega A_{\pm} \right|. \qquad \text{(A4b)}$$

Equation (A4a) implies that the amplitude of the wave does not change significantly over a distance of one wavelength λ, and Eq. (A4b) implies that the amplitude of the wave does not change significantly over a time duration of $1/\nu$. With these slowly varying amplitude approximations, Eq. (A3) reduces to

$$\frac{\partial A_{\pm}(x,t)}{\partial x} \mp \frac{1}{c}\frac{\partial A_{\pm}(x,t)}{\partial t} = 0. \qquad \text{(A5)}$$

This equation is the reduced wave equation referred to in the text.

REFERENCES

1. A. V. Okishev, W. Seka, J. H. Kelly, S. F. B. Morse, J. M. Soures, M. D. Skeldon, A. Babushkin, R. L. Keck, and R. G. Roides, in *Conference on Lasers and Electro-Optics*, *Vol. 11*, 1997 OSA Technical Digest Series (Optical Society of America, Washington, DC, 1997), p. 389.

2. Laboratory for Laser Energetics LLE Review **73**, 1, NTIS document No. DOE/SF/19460-212 (1997). Copies may be obtained from the National Technical Information Service, Springfield, VA 22161.

3. W. C. Johnson, *Transmission Lines and Networks*, 1st ed., McGraw-Hill Electrical and Electronic Engineering Series (McGraw-Hill, New York, 1950).

4. A. V. Okishev and W. Seka, IEEE J. Sel. Top. Quantum Electron. **3**, 59 (1997).

5. S. C. Burkhart and R. B. Wilcox, IEEE Trans. Microw. Theory Tech. **38**, 1514 (1990).